Test Results of Friction Factor for Round-Hole Roughness Surfaces in Closely Spaced Channel Flow of Water

Tae Woong Ha*
Associate professor, Mechanical Engineering Department, Kyungwon University, Sungnam, Korea, 461-701

For examining friction-factor characteristics of round-hole pattern surfaces which are usually applied on damper seals, flat plate test apparatus is designed and fabricated. The measurement method of leakage and pressure distribution along round-hole pattern specimen with different hole area is described and a method for determining the Fanning friction factor is discussed. Results show that the round-hole pattern surfaces provide a much larger friction factor than smooth surface, and the friction factor vs. clearance behavior yields that the friction factor generally decreases as the clearance increases unlike the results of Nava's flat plate test. As the hole depth is decreased, the friction factor is increased, and maximum friction factor is obtained for 50% of hole area. Since the present experimental friction factor results show coincident characteristics with Moody's friction factor model, empirical friction factors for round-hole pattern surfaces are obtained by using the Moody's formula based on curve-fit of the experimental data. Results of Villasmil's 2D CFD simulation support the present experimental test result.

Key Words: Friction Factor, Flat Plate Tester, Round-Hole Pattern Surface, Moody Friction Factor Model, Damper Seal

Nomenclature

A : Cross-sectional area (m^2)
a, b, c : Coefficients of Moody' friction factor model in Eq. (2)
c_l : Clearance of test section (m)
d : Hole depth (m)
D : Pipe diameter (m)
D_h : Hydraulic diameter in Eq. (4) (m)
e : Absolute roughness (m)
f : Fanning friction factor in Eq. (7)
f_B : Blasius model of friction factor in Eq. (1)
f_M : Moody model of friction factor in Eq. (2)
h_f : Pressure loss due to friction effect in Eq. (3) (Pa)
l : Total distance of △P (m)
△P : Pressure drop (Pa)
Q : Flow rate (m^3/s)
Re : Reynolds number in Eq. (6)
v : Flow velocity in Eq. (5) (m/s)
w : Width of test section (m)
γ : (hole area/total area) × 100(%)
μ : Fluid viscosity ($N-s/m^2$)
ρ : Fluid density (kg/m^3)
Φ : Hole diameter (m)

* **E-mail** : twha@kyungwon.ac.kr
TEL : +82-31-750-5308; **FAX** : +82-31-750-5273
Associate professor, Mechanical Engineering Department, Kyungwon University, Sungnam, Korea, 461-701. (Manuscript **Received** March 4, 2003; **Revised** July 30, 2004)

1. Introduction

The "damper-seal" for liquid annular seal is used to increase the efficiency and the stability of turbomachinery by employing a smooth rotor and deliberately roughened stator combination. The roughened stator is able to reduce the leakage and the circumferential velocity in the seal, thus yielding lower cross-coupled stiffness value than conventional smooth stator seals. Since Von Pragenau (1982) initially proposed a damper seal

configuration, various artificially roughened surface patterns, viz. knurled, diamond-grid, and round-hole roughness etc., have been designed and adopted for the optimum configurations [(Childs and Kim, 1985, 1986), (Iwatsubo and Sheng, 1990), (Childs et al., 1990), (Nava, 1993), (Childs and Fayolle, 1999)].

The round-hole roughness pattern has been widely used for the stator of damper seals in turbopumps. Childs and Kim(1986) measured leakage and effective stiffness and damping coefficients with various round-hole pattern damper seals. Childs and Kim's measurement showed that the round-hole pattern seal increases net damping by 37%, while reducing leakage by 46% comparing to a smooth seal. Childs et al. (1990) published test results of leakage, axial pressure gradients, friction factors, and rotordynamic coefficients for round-hole pattern damper seals with various hole area (Y) and hole-depth/clearance ratio (d/c_1). Childs et al.'s results showed that the round-hole pattern seals leak approximately one third less than the smooth seal. Childs and Fayolle (1999) also presented test results of leakage and rotordynamic coefficients for round-hole pattern damper seals. They provided a partial explanation for the experimental result of unexpectedly low direct stiffness by measured friction factor data.

Theoretical analysis for damper seals are generally based on Hirs'(1973) bulk-flow model. The bulk-flow model assumes that turbulence is accounted for entirely by shear stresses acting at the rotor and stator surfaces. The shear stresses are defined in terms of friction factor. Therefore, accurate predictions of leakage and rotordynamic coefficients for round-hole damper seals depend on the precise empirical friction-factor models for round-hole pattern surfaces. Blasius type friction-factor model of Eq. (1) and Moody friction-factor model of Eq. (2) are generally used in the theoretical analysis of damper seals. The Moody's friction-factor model defines a friction factor as a function of both Reynolds number (Re) and relative roughness (absolute roughness hydraulic diameter (e/D_h)). However, the Blasius type friction-factor model used by Hirs is defined as a function of Re only. Von Pragenau initially used the Moody's model for damper seal analysis. Nelson and Nguyen (1987) provided a comparison between damper seal analysis results using the Blasius and the Moody's model. The coefficient values of friction-factor models for damper seal surfaces, viz., n and m or a, b, and c, should be determined from experimental data by using a seal test rig. or a flat-plate tester.

$$f_B = n(Re)^m \tag{1}$$

$$f_M = a\left[1+\left(b\left(\frac{e}{D_h}\right)+\frac{c}{Re}\right)^{1/3}\right] \tag{2}$$

There have been a few investigations of friction factors for round-hole pattern surfaces. Childs et al. (1990) provided friction-factor data for round-hole pattern surface with 3.8mm hole diameter, 0.37mm clearance, 34% hole area, and 4 different hole depth. Childs et al. measured leakage and axial pressure profiles to determine the empirical coefficients of Blasius model with damper seal test rig. However, Childs et al. mentioned that measured friction factors showed serious deviations from the assumed Blasius friction factor model. Nava (1993) showed friction-factor data for round-hole pattern surface vs. smooth surface with two different recess sizes, viz., large recess (Φ=3.96mm, d=1.18mm, and Y=38%) and small recess (Φ=1.98mm, d=0.56mm, and Y=38%). Nava measured leakage and axial pressure profiles to calculate friction factor using a flat plate tester with several different clearances. Test results yielded the friction-factor plateau phenomena. For certain clearances the friction factor increased as the clearance increased. Then, the friction factor ceased to increase at a certain clearance and rather decreased as the clearance increased further. Childs and Fayolle (1999) published friction-factor data for round-hole pattern surfaces with 3.175mm hole diameter, 0.1mm and 0.12mm clearances, 44% hole area, and 0.28mm and 2.0mm hole depth. Childs and Fayolle's test results showed the increase in friction factor with increasing clearance. However, the pressure was only measured in inlet and outlet plenum, and no fair estimation on inlet and exit losses is possible in Childs and Fayolle's seal

experiments. Villasmil (2002) used a commercial computational fluid dynamics code to calculate the friction factor for round-hole pattern surfaces of narrow channel flow. Compared with the Nava's flat plate test results, Villasmil's theoretical results yielded over predictions up to 33~380% in friction factor and did not reproduce the friction factor vs. clearance behavior.

The present test program investigates the characteristics of friction factor for the round-hole pattern vs. smooth surface using a flat plate tester as a function of Y, d, cl, and Re. Nava and Childs and Fayolle's clearance behavior, which is the increase in friction factor with increasing clearance, is checked. The present research was stimulated from developing theoretical analysis for the round-hole damper floating ring seal [Ha et al., (2002)] of turbo-pumps, in which the knowledge of friction factor for round-hole surfaces is necessitated. A proper empirical friction factor model based on test results is suggested.

2. Test Apparatus

The flat plate test system [Ha et al., (2003)] is designed to measure flow rate, temperature, and static pressure gradient through the flat plate test specimen under the various test parameters. Fig. 1 shows the schematic of the friction-factor measurement system.

The flat plate tester, which is modeled after that of Ha and Childs (1992), consists of a test block (③, ④), a spacer, and a round-hole test specimen (⑥), as shown in Fig. 2, which is designed to permit the installation of various round-hole test specimens. To prevent side leakage, a 2mm diameter O-ring is positioned along the spacer. The round-hole pattern test specimen of Fig. 3 is made of brass. The holes are produced by a milling machine operation, have flat bottoms and nominally sharp edges. A reducer (①, 75mm × 50mm) welded on 200mm diameter flange (②) is attached at inlet and outlet of the test block assembly for keeping relatively larger cross-sectional area than that of flat plate tester.

Water of 5 bar controlled by a constant pressure supply system is supplied through 50mm diameter stainless steel pipe to flat plate tester from the pump. The pressure control valve is positioned downstream of the test section to control outlet pressure and flow condition of Reynolds number. The flow-rate through the test section is measured by 25mm diameter turbine flow meter, located in the upstream of test section. Resolution

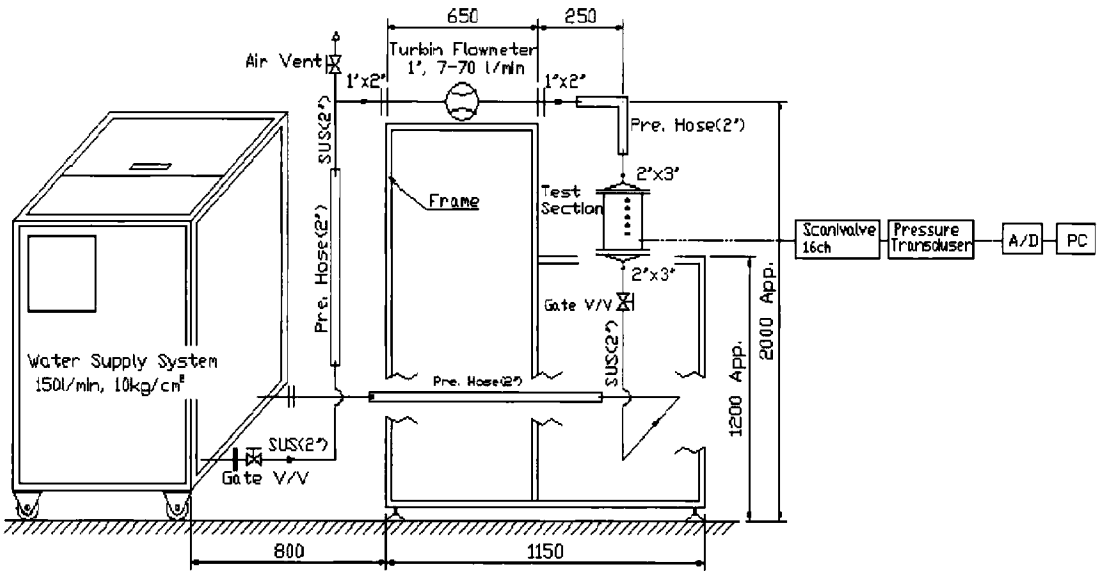

Fig. 1 Test facility schematic (unit : mm)

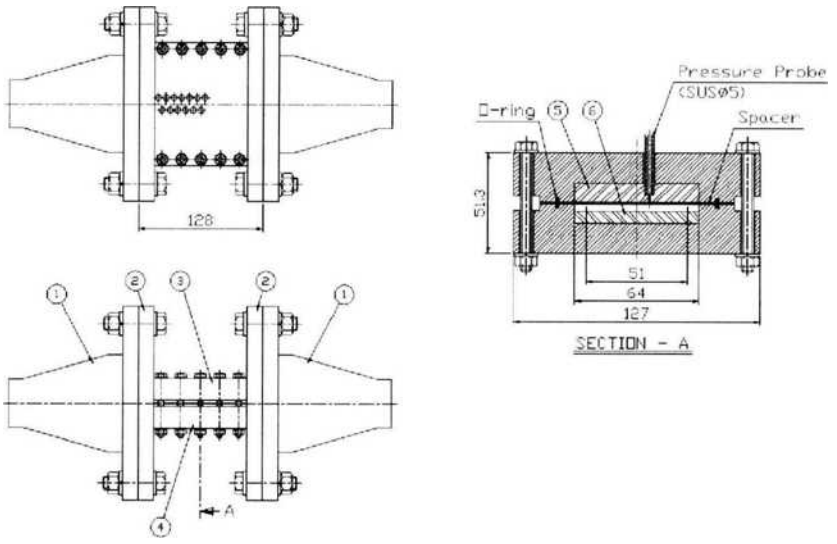

Fig. 2 Flat plate tester (unit : mm)

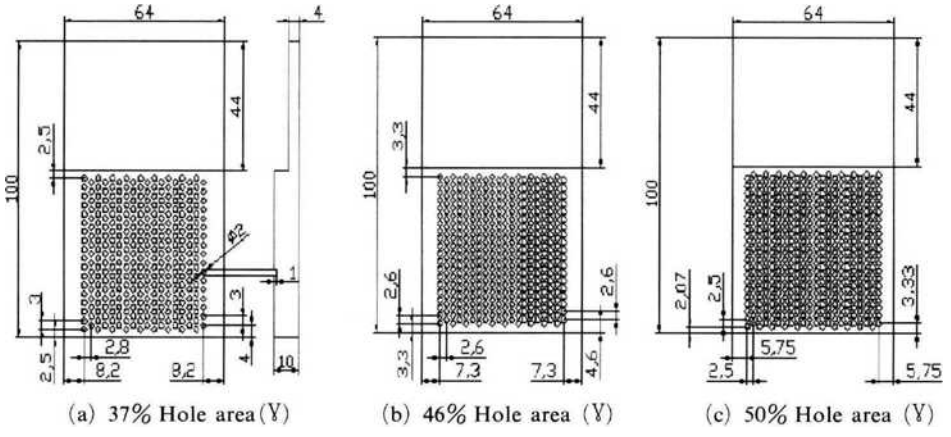

(a) 37% Hole area (Y) (b) 46% Hole area (Y) (c) 50% Hole area (Y)

Fig. 3 Typical round-hole pattern test specimen (unit : mm)

of the flow meter is $0.116\times10^{-4}(m^3/s)$. For measurement of the pressure distribution through the round-hole test specimen, upper test block with smooth specimen(⑤ in Fig. 2) has 13 pressure taps which are drilled along the length of the test specimen and equally distributed by 4mm intervals. The pressures are measured with a 0 to 7 bar Scani Valve differential-type pressure transducer through 16 channels. Pressure transducer's resolution is 0.56 kPa. The average temperature of inlet water is 293K and the resolution of temperature measurement is 1K.

3. Friction Factor Formula for Thin Channel Flow

For steady-incompressible-viscous flow driven by pressure in constant-circular parallel pipe, the friction head loss (h_f) is reduced to simple expression of Eq. (3). No external works or heat transfer effects are assumed. $\triangle P$ due to wall friction is stated for a pipe of length l in Eq. (3). The Fanning friction-factor(f) definition, which is introduced in the Hirs' bulk flow model of seal analysis, is used in Eq. (3) and differs by 4 from

the Darcy-Weisbach friction factor which are commonly used in the Moody diagram for pipe friction.

$$\triangle P=h_f=(4f)\frac{l}{D}\frac{\rho v^2}{2} \tag{3}$$

Since the thin rectangular channel flow of the flat plate tester is being modeled here, the pipe diameter D is replaced with the hydraulic diameter (D_h) of the rectangular cross sectional area. The width of test section is much larger than the clearance ($w \gg c_l$), therefore Dh reduces to the following expression of Eq. (4).

$$D_h=\frac{4A}{P_w}=\frac{4(w\times c_l)}{2\times(w+c_l)}\fallingdotseq 2\times c_l \tag{4}$$

Where P_w is the wetted perimeter and A is the test sectional area. The average flow velocity (v) for the rectangular test section is stated in Eq. (5), where Q is the volumetric flow rate. Re for the rectangular test section are defined using the hydraulic diameter as shown in Eq. (6), where ρ and μ are density and viscosity of water, respectively. Finally, a friction factor formula for the flat plate test, as shown in Eq. (7), is developed by substituting Eqs. (4) and (5) to Eq. (3).

$$v=\frac{Q}{(w\times c_l)} \tag{5}$$

$$Re=\frac{\rho D_h v}{\mu}=\frac{\rho(2\,c_l)\,v}{\mu} \tag{6}$$

$$f=\frac{\triangle P}{\rho}\frac{c_l^3}{l}\frac{w^2}{Q^2} \tag{7}$$

4. Data Reduction and Uncertainty in Friction Factors

Tests are carried out with smooth and round hole pattern test specimens as listed in Table 1. For each test case (viz. one particular ϒ, d, c_l, and Re), the test is performed three times and test data are averaged. Friction factor distribution along the test specimen can be determined using Eq. (7) since all of the variables are either known or measured. The friction factor distribution is averaged for a nominal friction factor of each test case.

Uncertainty in results of friction factor is determined using the Kline-McClintock method described by Holman (1978). The primary measurements in the friction factor calculations are clearance, width, length of △P, pressure, and flowrate as shown in Eq. (7). The uncertainties in these measurements are about 0.5×10^{-4}(m), 0.5×10^{-3}(m), 0.25×10^{-4}(m), 0.56(kPa), and 0.116×10^{-4}(m^3/s), respectively. As a result, the estimated maximum and minimum uncertainty in friction factor calculation are 10.39% and 3.24%.

5. Results and Discussion

For an examination of performance of the present flat plate tester, at first, pressure distributions are measured for smooth vs. smooth surface specimen with test conditions of inlet pressure=5.0bar, △P=3.11bar, and c_l=0.8mm. The plain seal analysis code developed by Ha and Lee (1998) is used to yield theoretical results. In

Table 1 List of test cases

Test No.	ϒ (%)	Φ (mm)	d (mm)	c_l (mm)	Range of Re	Range of f
1	37	2	1	0.2−0.8	2700−33000	0.0221−0.0127
2	46	2	1	0.2−0.8	1900−34000	0.0244−0.0131
3	50	2	1	0.2−0.8	1700−24000	0.0324−0.0170
4	37	2	0.75	0.2−0.8	1500−31000	0.0572−0.0179
5	46	2	0.75	0.2−0.8	1400−35000	0.0509−0.0148
6	50	2	0.75	0.2−0.8	1600−34000	0.0595−0.0193
7	50	2	0.3	0.2−0.8	2200−31000	0.1036−0.0206

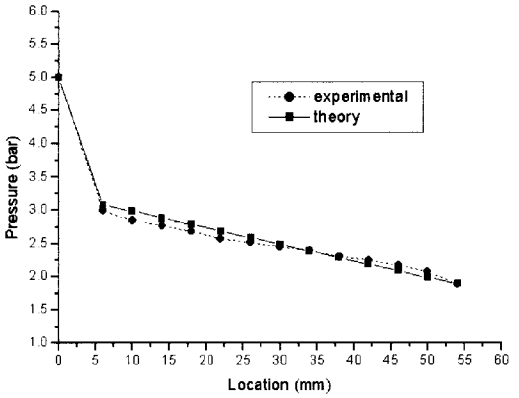

Fig. 4 Pressure distributions between experimental data and theoretical result for smooth surface ($\triangle P$=3.11bar)

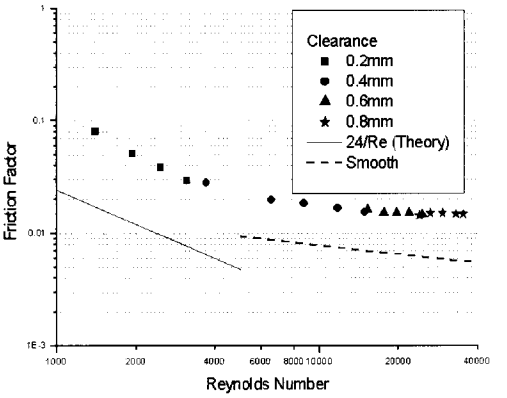

Fig. 5 Typical friction factor for round-hole pattern and smooth surface

theoretical analysis, the followings are assumed; (1) inlet loss coefficient=0.1, (2) circumferential velocity at the inlet=0, (3) n=0.079 and m=−0.25 for smooth surface friction factor of the Hirs' friction factor formula [Eq. (1)]. As shown in Fig. 4, sudden pressure drop or inlet loss occurs due to the large change of cross-sectional area at the seal inlet. The experimental pressure distribution and theoretical result yields a good agreement. The measured leakage of 0.9833(kg/s) is also closely matched with the predicted leakage of 0.9822(kg/s).

In the thin rectangular channel flow of the flat plate tester, there are three classical flow regions, viz., laminar, transition, and turbulent. According to Potter and Foss (1975), the laminar flow of the present flat plate test exists for Reynolds numbers, defined in Eq. (6), below 3,000 and never past 15,400. The Fanning friction factor for the laminar regime of the thin rectangular channel flow is theoretically defined as f=24/Re [Nava (1993)].

Figure 5 shows friction factor results for a typical round-hole pattern specimen (test No. 5). The Reynolds number range of 0.2mm clearance test lies in laminar flow regime and the friction factor illustrates relatively large slope against Reynolds number. The experimental friction factor line of laminar regime shows a similar slope but much higher than the theoretical laminar friction factor line of 24/Re. A similar experimental result in the flat plate test with round-hole pattern surfaces have been reported by Nava (1993) and this suggests that the hydraulic diameter definition of Eq. (4) used to drive the Reynolds number of Eq. (6) may not be appropriate for flow between closely spaced parallel plates. The Reynolds number ranges for 0.4mm, 0.6mm, and 0.8mm clearance tests lie transition or turbulent regime, and the friction factors decrease slightly as Reynolds number increases. Generally, the characteristics of friction factor vs. Reynolds number for round-hole pattern surfaces yields similarity as that for smooth pipe (dashed line in Fig. 5), viz., Moody diagram. The friction factor for round-hole pattern is much higher than that of smooth (e/D_h=0.0001) surface (dashed line in Fig. 5).

The Reynolds number range of 0.2mm clearance test for all round-hole pattern specimens is below about 3,000 and lies in laminar regime. Since the flow regime for the practical annular seal of turbomachinery lies in transition or turbulent regime, only results for Reynolds numbers over about 3,000, viz., 0.4mm, 0.6mm, and 0.8mm clearance tests, are presented and discussed in this paper.

Figures. (6)~(12) show experimental friction factor against Reynolds number with three different clearances for test No. (1)~(7), respectively. Table 1 also lists the range of experimental friction factor data and the range of Re. An inspection of these figures and Table 1 leads to the following conclusions:

(a) Since the Reynolds number ranges for 0.

4mm, 0.6mm, and 0.8mm clearance tests do not overlap in some cases, it is somewhat difficult to examine the clearance effect. However, the friction factor generally decreases as the clearance increases except test No. (1) and (6). Recall that at constant roughness height, an increase in clearance is equivalent to a reduction in the relative roughness. The present friction factor vs. clearance behavior shows an opposit trend compared with that of Nava's flat plate test. Recall that Nava's test results yielded that the friction factor increased as the clearance increased for certain clearance range.

(b) Comparing Fig. (8) [$\forall$=50%, d=1.0mm], (11) [$\forall$=50%, d=0.75mm] and (12) [$\forall$=50%, d=0.3mm], the friction factor slightly increases as the hole depth decreases. This trend is also maintained for the other hole-area cases of $\forall$=37% and $\forall$=46%.

(c) For 1.0mm hole depth cases, comparing Fig. (6) [$\forall$=37%], (7) [$\forall$=46%] and (8) [$\forall$=50%], the friction factor increases as the hole area ($\forall$) increases. viz., 37%<46%<50%. However, the hole area of 50% yields the largest friction factor followed by 37% and 46% in 0.75mm hole depth cases.

(d) The round-hole pattern of Φ=2mm, d=0.3mm, $\forall$=50%, test No. 7, yields the largest friction factor in the present tests.

The characteristics of friction factor defined by the Moody's friction factor model of Eq. (2) are that the friction factor decreases asymptotically as the Reynolds number increases, and also decreases if the relative roughness is decreased. The

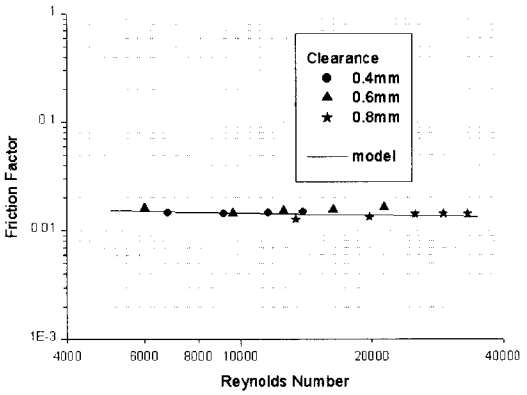

Fig. 6 Friction factor vs. Reynolds number for test No. 1

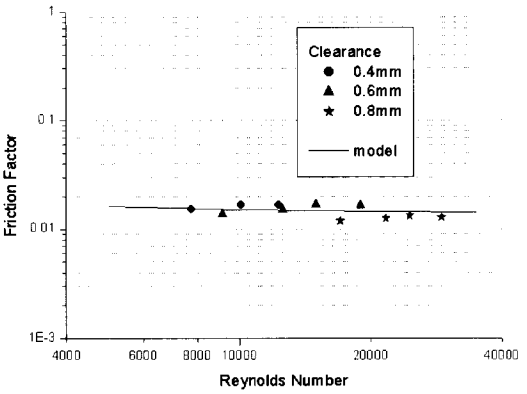

Fig. 7 Friction factor vs. Reynolds number for test No. 2

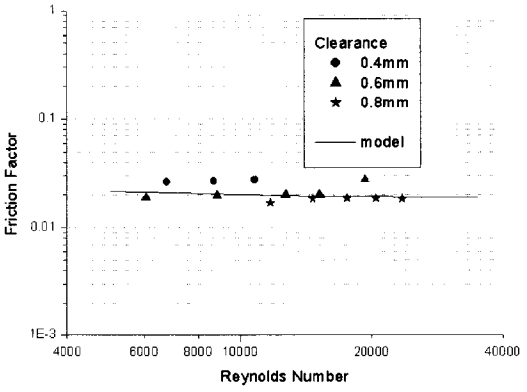

Fig. 8 Friction factor vs. Reynolds number for test No. 3

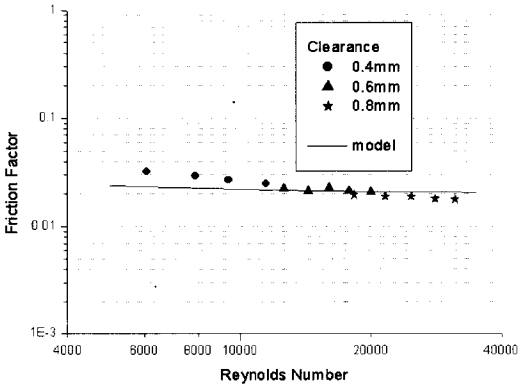

Fig. 9 Friction factor vs. Reynolds number for test No. 4

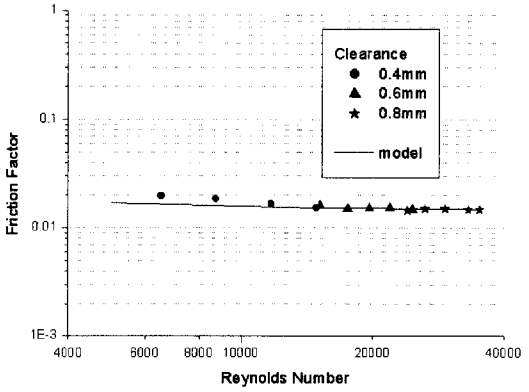

Fig. 10 Friction factor vs. Reynolds number for test No. 5

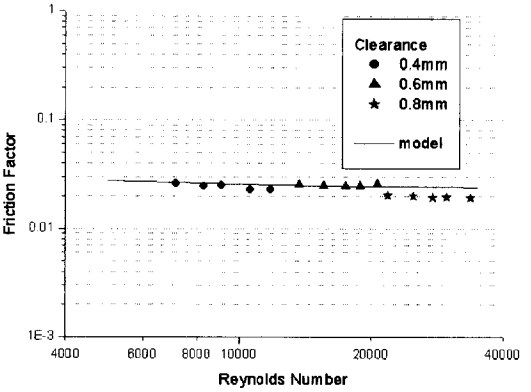

Fig. 11 Friction factor vs. Reynolds number for test No. 6

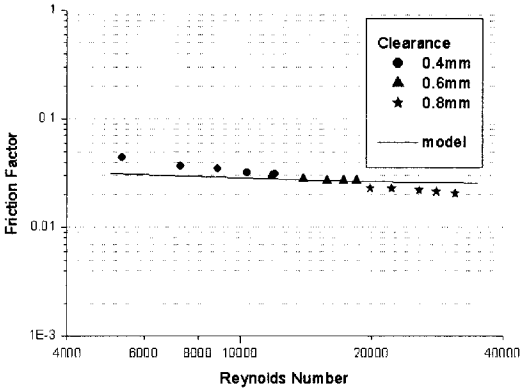

Fig. 12 Friction factor vs. Reynolds number for test No. 7

Table 2 Coefficients of Moody's friction factor formula for round-hole pattern surfaces

Test No.	a	b	c	$(e/D_h)_m$ for $c_{l=0.6mm}$
1	0.68×10^{-3}	2×10^{4}	2×10^{7}	0.3125
2	0.72×10^{-3}	2×10^{4}	2×10^{7}	0.3125
3	0.95×10^{-3}	2×10^{4}	2×10^{7}	0.3125
4	1.07×10^{-3}	2×10^{4}	2×10^{7}	0.2778
5	0.77×10^{-3}	2×10^{4}	2×10^{7}	0.2778
6	1.25×10^{-3}	2×10^{4}	2×10^{7}	0.2778
7	1.54×10^{-3}	2×10^{4}	2×10^{7}	0.1667

present experimental friction factor results show coincident characteristics with the Moody's friction factor model. Relative roughness is defined by the ratio absolute roughness height to the hydraulic diameter, $D_h=2\,c_l$. Since the absolute roughness is depth of hole for round-hole pattern surfaces, the geometrical relative roughness of round-hole surfaces becomes very large because of $d>c_l$, and thus has no meaning. Therefore, modified relative roughness$[(e/D_h)_m]$ is defined, instead of original $e/D_h=d/(2\,c_l)$, as shown in Eq. (8). A solid lines in Figs. (6) ~ (12) represent an empirical friction factor model defined by the Moody's formula with the modified relative roughness definition for 0.6mm clearance case of test No. (1) ~ (7), respectively. The empirically obtained coefficients of a, b, c, and $(e/D_h)_m$ for 0.6mm clearance are listed in Table 2.

$$(e/D_h)_m=\frac{d}{2(c_l+d)} \tag{8}$$

There have been two experimental and one theoretical published results to be compared with the present experimental friction factor for round-hole pattern surfaces, even though round hole geometries of those data are not exactly matched each other. Therefore, the close geometry test cases are selected and compared in Fig. 13. As shown in Table 3, the present test No. 4 and Nava's small recess have close test geometries, and also Childs and Fayolle, and Nava's large recess. The result of Villasmil's 2D computational fluid dynamics (CFD) code is for the Nava's small recess case.

Table 3 Test geometries for published round-hole pattern friction factors

Author	Y (%)	Φ (mm)	d (mm)	c_l (mm)	Remark
Test No. 4	37	2	0.75	0.6	Experiment
Nava's small recess	38	1.98	0.56	0.508	Experiment
Villasmil	38	1.98	0.56	0.508	Simulation
Nava's large recess	38	3.96	1.18	0.127	Experiment
Child and Fayolle	44	3.175	0.28	0.127	Experiment

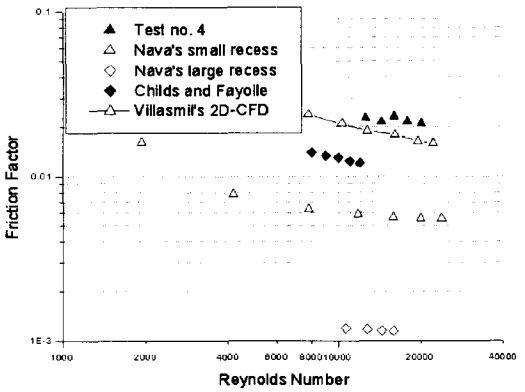

Fig. 13 Comparisons between present and published results

There are big differences in friction factor values between each pair of comparisons, even considering that their geometries are not exactly same. Nava's test results generally yield much lower value of friction factor than the present and the Childs and Fayolle's test results. The author can not clearly explain about 4 times discrepancy between the present and the Nava's result. However, if there were possible misunderstandings for the definition of friction factor between the Fanning's and the Darcy-Weisbach's model, Nava's results may be very close to the present results. Recall that the Darcy-Weisbach's friction factor is 4 times larger than that of Fanning. Villasmil's theoretical analysis over-predicts about 290% compared to Nava's experimental result for small recess case, while under-predicts about 78% compared to the present test result. Taking a little difference in geometries between Nava and the present test into account, result of Villasmil's 2D CFD simulation supports the present experimental test result.

7. Conclusion

A Flat plate tester is used to investigate the friction factor of round hole pattern surfaces. The measurement of leakage and pressure distribution through round-hole pattern specimens with three different hole areas, three hole depths, and four clearances is performed in the Reynolds number range of 1,400~35,000. The comparisons in the preceding results and discussion lead to the following conclusions:

(a) Generally, round-hole pattern surfaces provide a much larger friction factor than a smooth surface.

(b) The friction factor vs. clearance behavior for round-hole pattern surfaces shows that the friction factor generally decreases as the clearance increases unlike the result of Nava's flat plate test.

(c) As the hole depth of round-hole pattern decreases, the friction factor slightly increases.

(d) For 1.0mm hole depth cases, the friction factor increases as the hole area(Y) increases. viz., 37%<46%<50%. However, the hole area of 50% yields the largest friction factor followed by 37% and 46% for 0.75mm hole depth cases.

(e) The round-hole pattern with Φ=2mm, d=0.3mm, and Y=50% illustrates the largest friction factor in the present tests.

(f) Since the present experimental friction factor results show coincident characteristics with the Moody's friction factor model, an empirical friction factor for round-hole pattern surfaces is defined using the Moody's formula based on curve-fit of the experimental data.

(g) The result of Villasmil's 2D CFD simulation supports the present experimental test result.

References

Childs, D. W., and Kim, C.-H., 1985, "Analysis and Testing for Rotordynamic Coefficients of Turbulent Annular Seals with Different, Directionally-Homogeneous Surface-Roughness Treatment for Rotor and Stator Elements," *ASME Journal of Tribology*, Vol. 107, No. 3, pp. 296~

306.

Childs, D. W., and Kim, C.-H., 1986, "Test Results for Round-Hole-Pattern Damper Seals : Optimum Configurations and Dimensions for Maximum Net Damping," *ASME Journal of Tribology*, Vol. 108, pp. 605-611.

Childs, D. W., Nolan, S. A., and Kilgore, J. J., 1990, "Additional Test Results for Round-Hole-Pattern Damper seals : Leakage, Friction Factors, and Rotordynamic Force Coefficients," *ASME Journal of Tribology*, Vol. 112, pp. 365~371.

Childs, D. W., and Fayolle, P., 1999, "Test Results for Liquid "Damper" Seals using a Round Hole Roughness Pattern for the Stators," *ASME Journal of Tribology*, Vol. 121, pp. 42~49.

Ha, T. W., and Childs, D. W., 1992, "Friction-Factor Data for Flat Plate Tests of Smooth and Honeycomb Surfaces," *ASME Journal of Tribology*, Vol 114, pp. 722~730.

Ha, T. W. and Lee A. S., 1998, "A Modeling of Pump Impeller Shroud and Wear-Ring Seal as a Whole, and Its Application to the Pump Rotordynamics," *KSME International Journal*, Vol. 12, No. 3, pp. 441~450.

Ha, T. W., Lee, Y. B., and Kim, C. H., 2002, "Leakage and Rotordynamic Analysis of a High Pressure Floating Ring Seal in The Turbo Pump Unit of a Liquid Rocket Engine," *Tribology International*, Vol. 35, pp. 153~161.

Ha, T. W., Ju, Y. C., Lee, Y. B., and Kim, C. H., 2003, "Characteristics of Friction Factor for Artificially Roughened Surfaces," *Journal of Fluid Machinery*, Vol. 6, No. 3, pp. 15~20.

Hirs, G., 1973, "A Bulk-Flow Theory for Turbulence in Lubricant Films," *ASME Journal of Lubrication Technology*, pp. 137~146.

Holman, J. P., 1978, *Experimental Methods for Engineers*, McGraw-Hill, pp. 45.

Iwatsubo, T., and Sheng, B., 1990, "An Experimental Study on the Static and Dynamic Characteristics of Damp Seals," *in Proceedings of the Third IFToMM International Conference on Rotordynamics*, Lyon, france, pp. 307~312.

Nava, D. L., 1993, "Observation of Friction Factors for Various Roughness Patterns in Channel Flow," M.S. Thesis, Texas A&M University and Turbomachinery Laboratory Report No. TL-Seal-13-95.

Nelson, C., and Nguyen, D., 1987, "Comparison of Hirs' Equation with Moody's Equation for Determining Rotordynamic Coefficients of Annular Pressure Seals," *Journal of Tribology*, Vol 109, pp. 144~148.

Potter, M. C., and Foss, J. F., 1975, *Fluid Mechanics*, Okemos, MI, Great Lakes Press, pp. 282~284.

Villasmill, L. A., 2002, "Understanding The Friction Factor Behavior in Liquid Annular Seals with Deliberately Roughened Surfaces, A CFD Approach," M.S. Thesis, Texas A&M University.

Von Pragenau, G., 1982, "Damping Seals for Turbomachinery," NASA Technical Paper No. 1987.